Published as: *Cancer Discov*. 2012 November ; 2(11): 995–1003.

Androgen receptor signaling in circulating tumor cells as a marker of hormonally responsive prostate cancer

David T. Miyamoto[1,3,*], **Richard J. Lee**[1,4,*], **Shannon L. Stott**[2,5,*], **David T. Ting**[1,4], **Ben S. Wittner**[1], **Matthew Ulman**[1], **Malgorzata E. Smas**[1], **Jenna B. Lord**[1], **Brian W. Brannigan**[1], **Julie Trautwein**[1], **Neil H. Bander**[7], **Chin-Lee Wu**[6], **Lecia V. Sequist**[1,4], **Matthew R. Smith**[1,4], **Sridhar Ramaswamy**[1,4], **Mehmet Toner**[2,5], **Shyamala Maheswaran**[1,5], and **Daniel A. Haber**[1,4,8,**]

[1]Massachusetts General Hospital Cancer Center, Harvard Medical School, Charlestown, MA 02129

[2]Center for Bioengineering in Medicine, Harvard Medical School, Charlestown, MA 02129

[3]Department of Radiation Oncology, Harvard Medical School, Charlestown, MA 02129

[4]Department of Medicine, Harvard Medical School, Charlestown, MA 02129

[5]Department of Surgery, Harvard Medical School, Charlestown, MA 02129

[6]Department of Pathology, Harvard Medical School, Charlestown, MA 02129

[7]Weill-Cornell Medical College, New York-Presbyterian Hospital, New York, NY 10065

[8]Howard Hughes Medical Institute, Chevy Chase, MD 20815

Abstract

Androgen deprivation therapy (ADT) is initially effective in treating metastatic prostate cancer, and secondary hormonal therapies are being tested to suppress androgen receptor (AR) reactivation in castration-resistant prostate cancer (CRPC). Despite variable responses to AR pathway inhibitors in CRPC, there are no reliable biomarkers to guide their application. Here, we used microfluidic capture of circulating tumors cells (CTCs) to measure AR signaling readouts before and after therapeutic interventions. Single cell immunofluorescence analysis revealed predominantly “AR-on” CTC signatures in untreated patients, compared to heterogeneous (“AR-on, AR-off, and AR-mixed”) CTC populations in patients with CRPC. Initiation of first line ADT induced a profound switch from “AR-on” to “AR-off” CTCs, whereas secondary hormonal therapy in CRPC resulted in variable responses. Presence of “AR-mixed” CTCs and increasing “AR-on” cells despite treatment with abiraterone acetate were associated with an adverse treatment outcome. Measuring treatment-induced signaling responses within CTCs may help guide therapy in prostate cancer.

Keywords

androgen receptor; CTCs; prostate cancer; abiraterone acetate; castration resistance

** Corresponding authors Editorial Correspondence Dr. Daniel Haber Director, Cancer Center Massachusetts General Hospital Bldg 149, 13th Street Charlestown, MA 02129 Haber@helix.mgh.harvard.edu 617 726 7805 (tel) 617 724 6919 (fax).
*Denotes equal contribution

Conflict of Interest Statement: The authors disclose no conflicts of interests.

Introduction

Prostate cancer is highly dependent upon androgen receptor (AR) signaling for cell proliferation and survival. Androgen deprivation therapy (ADT) results in high rates of initial response in most patients with metastatic prostate cancer. However, disease progression is invariably observed with tumor cells resuming proliferation despite continued treatment (termed castration-resistant prostate cancer or CRPC) (1). The propensity of metastatic prostate cancer to spread to bone has limited repeated sampling of tumor deposits that have acquired castration resistance, but insights into resistance mechanisms have emerged through bone marrow biopsy and autopsy studies, as well as mouse modeling experiments (2). The concept that CRPC results from reactivation of AR signaling despite low levels of serum testosterone is consistent with a frequently observed rise in serum prostate specific antigen (PSA), an androgen-responsive gene product secreted into blood by prostate cancer cells (1, 2). Potential mechanisms by which AR reactivation occurs in CRPC include variable levels of AR gene amplification (~30% of cases), activating AR mutations, alternative mRNA splicing (~10%), increased expression or activation of AR transcriptional coactivators, activation of modulatory kinase pathways (e.g. Ras, PI3kinase), tyrosine phosphorylation of AR, and increased intratumoral androgen synthesis (see (2) for review). The functional significance of reactivated AR signaling in CRPC has been inferred from mouse xenograft models of prostate cancer, in which even modest increases in AR gene expression cause tumors to become resistant to castration (3).

The concept of AR reactivation in CRPC has become therapeutically relevant with the development of potent novel inhibitors of AR signaling (4, 5). The demonstration that abiraterone acetate, a CYP17A1 inhibitor that potently suppresses adrenal and intratumoral steroid biosynthesis, increases overall survival in men with metastatic CRPC who have previously received chemotherapy lends support to the rationale of suppressing AR reactivation in CRPC (5). Notably, there is a wide variation in patient response to abiraterone acetate as measured by serum PSA (5), and there is an unmet need for reliable biomarkers that can predict treatment response to abiraterone acetate and other potent inhibitors of AR signaling under development. Taking advantage of recent technological advances in the capture, imaging, and molecular characterization of rare CTCs shed into blood from otherwise poorly accessible metastatic tumor deposits (6, 7), we established a noninvasive “real time” measure of intratumoral AR signaling before and after initial or second line hormonal therapy in metastatic prostate cancer patients.

Results

Single cell measurement of AR signaling parameters in prostate CTCs

To measure the status of AR signaling within individual cells, we established a quantitative immunofluorescence assay based on the expression of AR regulated genes. We reasoned that such a readout would be independent of mechanisms of AR reactivation in CRPC (e.g. AR amplification or mutation, ligand overexpression, or AR cofactor misregulation) and would therefore provide a clear measure of whether the AR pathway has been re-activated during the acquisition of resistance to androgen deprivation therapy. To identify optimal downstream readouts of AR signaling, we subjected a prostate cancer cell line (LNCaP cells) to androgen deprivation or stimulation, and used digital gene expression (DGE) profiling to identify transcripts that are differentially regulated in response to changes in AR signaling (Supplemental Figure S1). Among candidate gene products that are prostate cancer specific and for which reliable antibodies are available, we selected Prostate Specific Antigen (PSA; KLK3) and Prostate Specific Membrane Antigen (PSMA; FOLH1) as most consistently upregulated following AR activation and AR suppression, respectively (Fig. 1a

and 1b; Supplemental Figure S1a and S1b). Selection of PSMA as a marker of AR suppression was also recently described by Evans et al. while this work was in progress (8).

Our assay for quantitative measurement of signal intensity profiles for cells stained with antibodies against PSA and PSMA was developed using a model cell system (LNCaP). Treatment of androgen-starved LNCaP cells with the androgen R1881 and measurement of immunofluorescence signals using an automated fluorescence microscopy scanning platform revealed time-dependent progression from an initial "AR-off" (PSA-/PSMA+) to an intermediate "AR-mixed" (PSA+/PSMA+) phenotype, and finally to an "AR-on" (PSA+/PSMA-) pattern (Fig. 1c; Supplemental Fig. S2a). The reverse progression was observed upon treatment with the AR inhibitor bicalutamide (Fig. 1d; Supplemental Fig. S2b). Similar results were observed using VCaP cells, another androgen responsive prostate cancer cell line (Supplemental Fig. S3).

For isolation of circulating tumor cells (CTCs), we made use of our recently developed "second generation" microfluidic chip, in which Herringbone (HB) grooves in the ceiling of the channel create anisotropic flow conditions, generating microvortices that direct cells toward the anti-EpCAM antibody coated walls of the device (^{HB}CTC-Chip) (7). ^{HB}CTC-Chip parameters for single cell AR signaling analysis were first established by modeling LNCaP cells treated with R1881 or bicalutamide, spiked into control blood specimens, captured on the ^{HB}CTC-Chip, and stained with antibodies against PSA and PSMA (AR signaling) along with anti-CD45 (to exclude contaminating leukocytes) and DAPI (nuclear morphology) (Supplemental Fig. S4a and S4b). To achieve multiparameter single cell analysis of AR activity, an automated fluorescence microscopy scanning platform was adapted to distinctly and specifically measure four fluorescent emission spectra simultaneously. We carefully selected the choice of secondary fluorophores and optical band pass filters to avoid "cross-talk" between the multiple fluorescent signals that are closely located on the electromagnetic spectrum, while maximizing signal intensity (see Methods). The four-color immunofluorescence imaging parameters established using LNCaP cells were then applied to accurately enumerate patient-derived CTCs (Fig. 2a). To minimize the risk of counting false positive events as CTCs, we adopted a previously reported strategy (6), calibrating threshold signal intensity and setting a cut-off value for detection of CTCs, based on the number of positive events detected in healthy donor samples. Using the newly optimized four-color immunofluorescence imaging parameters, we established a threshold value for positive CTC detection of >4 PSA+ or PSMA+/CD45- cells/mL, which was higher than any count noted in any healthy donor sample (Supplemental Fig. S5). The expansion of our CTC characterization to include four-color staining in a high throughput manner required the use of new organic fluorophores, narrow band fluorescent filter cubes, and a new automated imaging platform (see Methods). The result was a more specific assay with less background signal in our healthy donors in comparison to our previous papers (6, 7). We tested the validity of this threshold cut-off value in a separate cohort of age-matched male patients with no known diagnosis of cancer. Using this threshold, CTCs were not detectable in any patients without a diagnosis of prostate cancer (N = 0/21) (Supplemental Fig. S5). In contrast, subsequent analysis of pretreatment blood samples from patients with metastatic prostate cancer revealed detectable CTCs above the predetermined threshold cut-off in 72% of patients (N = 18/25) (Supplemental Fig. S5 and Supplemental Table S1).

Active AR signaling in CTCs from untreated patients with metastatic prostate cancer

Having standardized CTC detection using four color imaging criteria, we applied the PSA/PSMA dual immunophenotyping assay to patients with newly diagnosed metastatic prostate cancer. CTCs were detectable in 4 of 5 (80%) patients with newly diagnosed metastatic prostate cancer prior to the initiation of androgen deprivation therapy. AR activity was predominantly positive amongst the patients with detectable CTCs, with the vast majority

(median 99.1%, range 75%-100%) of isolated CTCs from each patient showing the "AR-on" (PSA+/PSMA-) phenotype (Figs. 2b and 2c; Supplemental Table S2). The initiation of ADT in treatment-naïve metastatic prostate cancer patients with detectable CTCs resulted in transformation of the majority of CTCs from the "AR-on" to the "AR-off" phenotype within one month, followed by the complete disappearance of CTCs by 3 months after initiation of therapy (Fig. 3a-c; Supplemental Table S2).

Heterogeneous AR signaling in CTCs from patients with CRPC

In marked contrast, CRPC patients with detectable CTCs pretreatment (N = 14/20; 70%) displayed both intra-patient and inter-patient heterogeneity in CTC AR activity (Fig. 2; Supplemental Table S2). Most remarkable was the abundance within each patient of CTCs with the "AR-off" (PSA-/PSMA+) signature (median 51.9%), as well as CTCs with an "AR-mixed" (PSA+/PSMA+) phenotype (median 17.6%). Despite the expected reactivation of AR signaling in CRPC, only a relatively small fraction of CTCs in these patients had the "AR-on" (PSA+/PSMA-) phenotype (median 11.1%). In contrast to the consistent treatment induced changes in AR signaling patterns seen within CTCs of patients with CSPC, second line hormonal treatment in CRPC patients had varying effects on CTC numbers and AR phenotypes (Fig. 4; Supplemental Tables S1 and S2). This included patients treated with the relatively weak hormonal agents ketoconazole (N=1) and bicalutamide (N=2), as well as the potent CYP17A1 inhibitor abiraterone acetate (N=17) (Supplemental Table S2). Four of 17 (24%) CRPC patients treated with abiraterone acetate had a ≥50% decline in the percentage of "AR-on" CTCs within 2-5 weeks of therapy, suggesting that the reduction in systemic androgen levels may have suppressed a subset of metastatic tumor cells with reactivated AR signaling (Fig. 4a-c; Supplemental Tables S1 and S2). In contrast, 2 of 17 (12%) CRPC patients had a ≥2-fold increase in the percentage of "AR-on" CTCs within the first 2-5 weeks of therapy with abiraterone acetate, suggesting increased AR signaling despite therapy (Fig. 4d-f; Supplemental Tables S1 and S2). Eleven of 17 (65%) CRPC patients had a stable percentage of "AR-on" CTCs after therapy. Analysis of baseline CTC AR signaling prior to the initiation of abiraterone acetate therapy suggested that the presence of a >10% component of "AR-mixed" CTCs was associated with decreased overall survival (logrank $P < 0.05$; Fig. 4g). In addition, an increase in the percentage of "AR-on" CTCs despite abiraterone acetate therapy was correlated with decreased overall survival (Supplemental Fig. S6).

Discussion

Cancer cells circulating in the peripheral blood provide a uniquely accessible source of tumor-derived material for molecular analyses. In metastatic prostate cancer, which primarily spreads to bone, the inability to noninvasively sample metastatic lesions has limited the ability to individualize second line therapies according to mechanism of drug resistance. Thus, while potent new inhibitors of the AR pathway are under active development, their clinical deployment still remains empiric. Given the inter-patient variation in outcome, there is an unmet clinical need for biomarkers that may enable prediction of treatment response for individual patients. Here, we show that the activity of the AR pathway may be monitored in CTCs. Although the trends we observe need confirmation in subsequent analysis with additional patients, our results support the relevance of CTCs as dynamic tumor-derived biomarkers, reflecting "real time" effects of cancer drugs on their therapeutic targets, and the potential of CTC signaling analysis to identify the early emergence of resistance to therapy.

Although CTC enumeration using immunomagnetic bead capture has previously been shown to be a potential prognostic biomarker in patients with metastatic prostate cancer (9), enumeration alone does not yield direct insight into the effects of drugs on their molecular

targets, and may simply reflect relative tumor burden or leakiness of tumor-associated vasculature. In contrast, interrogation of the activity of specific signaling pathways within CTCs may reveal whether targeted therapies are effectively hitting their target *in vivo*, thus providing information that may be useful in guiding therapeutic decisions. RT-PCR of transcripts from CTC-enriched cell populations may provide an alternative method for detecting CTCs (10), with the potential for measuring changes in relevant transcriptional output in CTCs. However, the need for quantitative analysis of signal within heterogeneous cell populations, as documented here, supports the importance of single cell measurements based on CTC imaging.

Since PSMA is a cell surface protein, it has been used as an alternative to EpCAM for capture of CTCs from patients with prostate cancer (11). While more specific to prostate cancer, PSMA-based capture may miss the “AR-on” subsets of CTCs, whose phenotype is primarily PSA+/PSMA- , and which may be important in defining response to hormonal therapies. As such, anti-EpCAM antibody-mediated capture followed by immunophenotyping for PSA versus PSMA expression allows for broad capture of CTCs, followed by characterization of their AR signaling status. Critical for this approach is the optimization of four-color immunofluorescence staining and imaging parameters, maximizing immunofluorescence signals, while minimizing cross-talk between channels for detection of PSA, PSMA, CD45, and nuclear signals, using a standardized semi-automated microscopy platform. Full automation of this assay will be required for its broad application in the context of clinical trials of novel hormonal agents in CRPC.

While our study was designed as a “proof of concept” for a diagnostic approach, it also provides significant insight into the evolution of initially responsive prostate cancer into castration-resistant disease. We found that profound differences underlie the dramatic response of previously untreated, castration-sensitive disease to androgen deprivation therapy, compared with the relatively limited effectiveness of even potent second line hormonal agents in castration-resistant disease. CSPC is marked by the presence of predominant and strong “AR-on” CTC signals, with rapid switching to “AR-off” upon androgen withdrawal, preceding the disappearance of CTCs from the circulation. In contrast, CRPC is marked by striking heterogeneity among tumor cells from individual patients, as well as between different patients with similar clinical histories. Few “AR-on” cells are observed, and instead there is an abundance of both “AR-off” and “AR-mixed” CTCs. Together, these suggest that pathways other than AR signaling contribute to disease progression in CRPC, and that the AR reactivation that does occur may be qualitatively altered despite the known overexpression of AR itself. Indeed, reactivation of AR signaling in CRPC does not appear to be as complete as previously suspected, and even potent AR suppression in this setting may be insufficient by itself to mediate dramatic tumor responses. Rising serum PSA levels in patients with CRPC have been taken as evidence of strong AR reactivation and potentially renewed susceptibility to hormonal manipulation. However, these serum measurements reflect total tumor burden, which may be considerable, whereas single cell CTC analysis suggests that within individual tumor cells, AR signaling is not fully reactivated.

While AR reactivation is the dominant model to explain acquisition of resistance to androgen withdrawal, the limited human data available are consistent with our observations of an attenuated AR phenotype in CRPC. For instance, gene expression studies of bone metastases have shown increased AR mRNA levels in CRPC (12), and bone marrow biopsy studies (13) as well as CTC analyses (14) have demonstrated nuclear AR localization in resistant disease. However, expression levels of androgen-activated genes appear to be reduced by 2- to 3- fold in CRPC, compared with primary untreated prostate cancer (12, 15). The most common acquired genetic alteration affecting AR, a median 1.6 to 5–fold gene

amplification seen in ~30% of cases (16, 17), may not be sufficient to fully overcome the effects of ligand withdrawal and re-establish full AR-driven tumor cell proliferation. Indeed a recent analysis of gene promoters targeted by AR in cells that are sensitive to androgen withdrawal versus cells with acquired resistance demonstrated a qualitatively distinct subset of AR activated genes (18, 19). In our study, the complexity of AR signaling pathways in CRPC may be reflected by the presence of "AR-mixed" CTCs, having simultaneous expression of androgen-induced and androgen-suppressed markers, which was associated with decreased overall survival. Thus, expression analysis of AR target genes within CTCs may provide functionally relevant measures of aberrant AR activity.

In addition to altered AR signaling, AR-independent pathways including PIK3CA-dependent signaling, have also been implicated in CRPC and may cooperate with partial AR reactivation in mediating disease progression in prostate cancer (20). Recent studies in mouse models of CRPC have suggested improved responses to combined AR and mTOR pathway inhibition (20). Given the potentially complex and heterogeneous mechanisms underlying CRPC, it is not surprising that treatment with the potent CYP-17A1 inhibitor abiraterone acetate alone has a varied effect on the number and composition of CTCs. Some CRPC patients who did have measureable "AR-on" CTCs demonstrated a >50% decline in the percentage of this CTC subset within 2-5 weeks of abiraterone acetate therapy (4 of 17 patients; 24%). Given the mechanism of drug action, these cases may be enriched for patients in whom intra-tumoral or adrenal gland synthesis of androgens plays a major role in the development of castration-resistance. In contrast, tumors driven by ligand-independent AR gene activation would not be expected to show any suppression in "AR-on" CTC numbers. Indeed, a rising fraction of "AR-on" CTCs despite continued abiraterone acetate therapy was associated with a poor outcome, defined as decreased overall survival. In these patients, ligand-independent AR activity may become a driver of tumor cell proliferation, leading to therapeutic failure. Potential mechanisms for the development of resistance to abiraterone acetate in CRPC are the subject of intense investigation (21). Further studies linking such mechanistic insights with the application of novel therapies targeting the relevant pathways may provide critical guidance in molecularly targeted therapy for CRPC.

In summary in this exploratory study, we show that PSA/PSMA-based AR signaling assay in CTCs* may enable real time quantitative monitoring of intra-tumoral AR signaling and its potential contribution to disease progression within an individual patient. Although this assay has potential as a promising biomarker, it requires validation in larger prospective studies of prostate cancer patients undergoing second-line hormonal therapy. While this work was in progress, PET imaging using radio-labeled antibodies against PSMA and PSA were reported as biomarkers of androgen receptor signaling in prostate cancer mouse xenografts treated with the investigational AR inhibitor MDV 3100 (8, 22). If successful in human tumor imaging, radioisotope scanning for AR activity may complement single cell CTC assays in providing ongoing monitoring for second line hormonal agents in CRPC. Such individualization of second line treatments in metastatic prostate cancer will be essential for therapeutic success, given the evident tumor cell heterogeneity that accompanies the emergence of resistance to initial androgen deprivation.

*In memory of Charles Evans and in recognition of philanthropic support for prostate cancer research from the Evans Foundation, we propose that this CTC-based test be called the Evans Assay.

Methods

Patients and Clinical Specimens

Metastatic prostate cancer patients receiving treatment at the Massachusetts General Hospital (MGH) were recruited according to an institutional review board (IRB)-approved protocol. Eligibility criteria included a histologic diagnosis of prostate adenocarcinoma and radiographic evidence of metastatic disease. For the CSPC cohort, recipients of prior hormonal therapy were excluded. Patients in the CRPC cohort required disease progression on ADT according to Prostate Cancer Working Group criteria (23), and may have received other therapies. A total of 25 patients donated 10-20 mL of blood on one or more occasions for CTC analysis. In addition, 21 male patients with no known diagnosis of cancer were recruited as controls using a separate IRB-approved protocol.

Cell Lines

LNCaP and VCaP cells were obtained from ATCC after authentication by Short Tandem Repeat profiling, and maintained as recommended. For generation of the AR signature, cells were cultured for 3 days in medium containing 10% charcoal-stripped fetal bovine serum (Invitrogen) and treated with R1881 (Perkin-Elmer), bicalutamide (Sigma), or DMSO as a vehicle control.

Immunofluorescence Staining and Automated Fluorescence Microscopy

Cells were captured on the ^{HB}CTC-chip as described (7), fixed and permeabilized as described (7), and stained with antibodies against PSA (rabbit polyclonal; DAKO), PSMA (J591 mouse monoclonal IgG1; N. Bander), and CD45 (mouse monoclonal IgG2a; Abcam), followed by appropriately matched secondary antibodies conjugated with DyLight 649 (Jackson ImmunoResearch), Alexa Fluor 555 (Invitrogen), and Alexa Fluor 488 (Invitrogen). Nuclei were stained with DAPI. An automated fluorescence microscopy scanning system (BioView) comprehensively imaged ^{HB}CTC-chips under 10X magnification in seven z-planes in four colors at predetermined optimized exposure times, using modified Magnetron sputter-coated filter sets for the Cy3 and Cy5 spectra (Chroma) (see Supplemental Methods for details). Potential CTCs were automatically classified using a previously described algorithm (6), followed by manual validation by a blinded human reviewer. High resolution immunofluorescence images were obtained using an upright fluorescence microscope (Eclipse 90i, Nikon) under 60X magnification.

Quantitative Single Cell Immunofluorescence Analysis

Quantitative fluorescence intensity data for emission spectra (DAPI, FITC, Cy3, and Cy5) were obtained for each single cell as “Area pixels” measurements using image analysis software (Bioview). Data files were converted to CSV format and to FCS format (TextToFCS version 1.2.1 (24)), and analyzed using FlowJo version 7.6. Pseudocolor density plots were gated to display events that are CD45 negative. Bar graphs were generated using Microsoft Excel reflecting proportions of PSA+/PSMA-/CD45-, PSA+/PSMA+/CD45-, and PSA-/PSMA+/CD45- CTCs tabulated after manual validation. Normalized counts (CTC/mL) were calculated by dividing the total CTC count by the total blood volume processed. A signal intensity threshold of detection based on healthy donors was determined to be 4 CTC/mL (Supplement Figure S5). Normalized counts below this threshold were considered false positive events and not included in the final analyses. In cases where normalized CTC counts were below the limit of reliable detection, percentage distributions of AR signaling phenotypes were not calculated (Supplemental Table S1).

Statistical Analysis

AR activity and the proportion of CTC phenotypes between samples were compared using the Wilcoxon rank-sum test. Overall survival was defined as the interval between the start of therapy and the date of death or censor. Serum PSA response was defined as a maximal decline of ≥50% in serum PSA (23). Survival curves were generated using the Kaplan-Meier method and compared using the log-rank test. Two-sided *P*-values <0.05 were considered statistically significant. Statistical analyses were performed using R, version 2.12.0.

Supplementary Material

Refer to Web version on PubMed Central for supplementary material.

Acknowledgments

This work was supported by a Challenge Grant from the Evans Foundation and the Prostate Cancer Foundation (PCF); a Stand Up To Cancer Dream Team Translational Research Grant, a Program of the Entertainment Industry Foundation (SU2C-AACR-DT0309); T.J. Martell Foundation (D.A.H.); Starr Cancer Consortium (D.A.H.); NIH-NIBIB-5R01EB008047 (M.T.); NCI-CA129933 (D.A.H.); NCI-C06-CA-059267 (D.T.M.); NIH-5K12CA87723-09 (D.T.T.); Department of Defense Physician Research Training Awards (D.T.M., R.J.L), Mazzone-DF/HCC Career Development Award (D.T.M.); Conquer Cancer Foundation Career Development Award and PCF Young Investigator Award (R.J.L.), American Cancer Society (S.L.S.); and Howard Hughes Medical Institute (D.A.H.). We thank J. Walsh, F. Floyd, G. Korir, C. Koris, and L. Libby for technical support.

References

1. Scher HI, Sawyers CL. Biology of progressive, castration-resistant prostate cancer: directed therapies targeting the androgen-receptor signaling axis. J Clin Oncol. 2005; 23:8253–61. [PubMed: 16278481]
2. Yuan X, Balk SP. Mechanisms mediating androgen receptor reactivation after castration. Urol Oncol. 2009; 27:36–41. [PubMed: 19111796]
3. Chen CD, Welsbie DS, Tran C, Baek SH, Chen R, Vessella R, et al. Molecular determinants of resistance to antiandrogen therapy. Nat Med. 2004; 10:33–9. [PubMed: 14702632]
4. Tran C, Ouk S, Clegg NJ, Chen Y, Watson PA, Arora V, et al. Development of a second-generation antiandrogen for treatment of advanced prostate cancer. Science. 2009; 324:787–90. [PubMed: 19359544]
5. de Bono JS, Logothetis CJ, Molina A, Fizazi K, North S, Chu L, et al. Abiraterone and increased survival in metastatic prostate cancer. N Engl J Med. 2011; 364:1995–2005. [PubMed: 21612468]
6. Stott SL, Lee RJ, Nagrath S, Yu M, Miyamoto DT, Ulkus L, et al. Isolation and characterization of circulating tumor cells from patients with localized and metastatic prostate cancer. Sci Transl Med. 2010; 2:25ra3.
7. Stott SL, Hsu CH, Tsukrov DI, Yu M, Miyamoto DT, Waltman BA, et al. Isolation of circulating tumor cells using a microvortex-generating herringbone-chip. Proc Natl Acad Sci U S A. 2010; 107:18392–7. [PubMed: 20930119]
8. Evans MJ, Smith-Jones PM, Wongvipat J, Navarro V, Kim S, Bander NH, et al. Noninvasive measurement of androgen receptor signaling with a positron-emitting radiopharmaceutical that targets prostate-specific membrane antigen. Proc Natl Acad Sci U S A. 2011; 108:9578–82. [PubMed: 21606347]
9. Danila DC, Heller G, Gignac GA, Gonzalez-Espinoza R, Anand A, Tanaka E, et al. Circulating tumor cell number and prognosis in progressive castration-resistant prostate cancer. Clin Cancer Res. 2007; 13:7053–8. [PubMed: 18056182]
10. Helo P, Cronin AM, Danila DC, Wenske S, Gonzalez-Espinoza R, Anand A, et al. Circulating prostate tumor cells detected by reverse transcription-PCR in men with localized or castration-refractory prostate cancer: concordance with CellSearch assay and association with bone metastases and with survival. Clin Chem. 2009; 55:765–73. [PubMed: 19233911]

11. Kirby BJ, Jodari M, Loftus MS, Gakhar G, Pratt ED, Chanel-Vos C, et al. Functional characterization of circulating tumor cells with a prostate-cancer-specific microfluidic device. PLoS One. 2012; 7:e35976. [PubMed: 22558290]
12. Stanbrough M, Bubley GJ, Ross K, Golub TR, Rubin MA, Penning TM, et al. Increased expression of genes converting adrenal androgens to testosterone in androgen-independent prostate cancer. Cancer Res. 2006; 66:2815–25. [PubMed: 16510604]
13. Efstathiou E, Titus M, Tsavachidou D, Tzelepi V, Wen S, Hoang A, et al. Effects of Abiraterone Acetate on Androgen Signaling in Castrate-Resistant Prostate Cancer in Bone. J Clin Oncol. 2011
14. Darshan MS, Loftus MS, Thadani-Mulero M, Levy BP, Escuin D, Zhou XK, et al. Taxane-induced blockade to nuclear accumulation of the androgen receptor predicts clinical responses in metastatic prostate cancer. Cancer Res. 2011; 71:6019–29. [PubMed: 21799031]
15. Mendiratta P, Mostaghel E, Guinney J, Tewari AK, Porrello A, Barry WT, et al. Genomic strategy for targeting therapy in castration-resistant prostate cancer. J Clin Oncol. 2009; 27:2022–9. [PubMed: 19289629]
16. Visakorpi T, Hyytinen E, Koivisto P, Tanner M, Keinanen R, Palmberg C, et al. In vivo amplification of the androgen receptor gene and progression of human prostate cancer. Nat Genet. 1995; 9:401–6. [PubMed: 7795646]
17. Brown RS, Edwards J, Dogan A, Payne H, Harland SJ, Bartlett JM, et al. Amplification of the androgen receptor gene in bone metastases from hormone-refractory prostate cancer. J Pathol. 2002; 198:237–44. [PubMed: 12237884]
18. Wang Q, Li W, Zhang Y, Yuan X, Xu K, Yu J, et al. Androgen receptor regulates a distinct transcription program in androgen-independent prostate cancer. Cell. 2009; 138:245–56. [PubMed: 19632176]
19. Cai C, He HH, Chen S, Coleman I, Wang H, Fang Z, et al. Androgen receptor gene expression in prostate cancer is directly suppressed by the androgen receptor through recruitment of lysine-specific demethylase 1. Cancer Cell. 2011; 20:457–71. [PubMed: 22014572]
20. Carver BS, Chapinski C, Wongvipat J, Hieronymus H, Chen Y, Chandarlapaty S, et al. Reciprocal feedback regulation of PI3K and androgen receptor signaling in PTEN-deficient prostate cancer. Cancer Cell. 2011; 19:575–86. [PubMed: 21575859]
21. Cai C, Chen S, Ng P, Bubley GJ, Nelson PS, Mostaghel EA, et al. Intratumoral de novo steroid synthesis activates androgen receptor in castration-resistant prostate cancer and is upregulated by treatment with CYP17A1 inhibitors. Cancer Res. 2011; 71:6503–13. [PubMed: 21868758]
22. Ulmert D, Evans MJ, Holland JP, Rice SL, Wongvipat J, Pettersson K, et al. Imaging androgen receptor signaling with a radiotracer targeting free prostate-specific antigen. Cancer Discovery. 2012; 2:320–7. [PubMed: 22576209]
23. Scher HI, Halabi S, Tannock I, Morris M, Sternberg CN, Carducci MA, et al. Design and end points of clinical trials for patients with progressive prostate cancer and castrate levels of testosterone: recommendations of the Prostate Cancer Clinical Trials Working Group. J Clin Oncol. 2008; 26:1148–59. [PubMed: 18309951]
24. http://offsite.treestar.com/downloads/utilities/TextToFCS_documentation

Significance

Acquired resistance to first line hormonal therapy in prostate cancer is heterogeneous in the extent of androgen receptor pathway reactivation. Measurement of pre and post treatment AR signaling within CTCs may help target such treatments to patients most likely to respond to second line therapies.

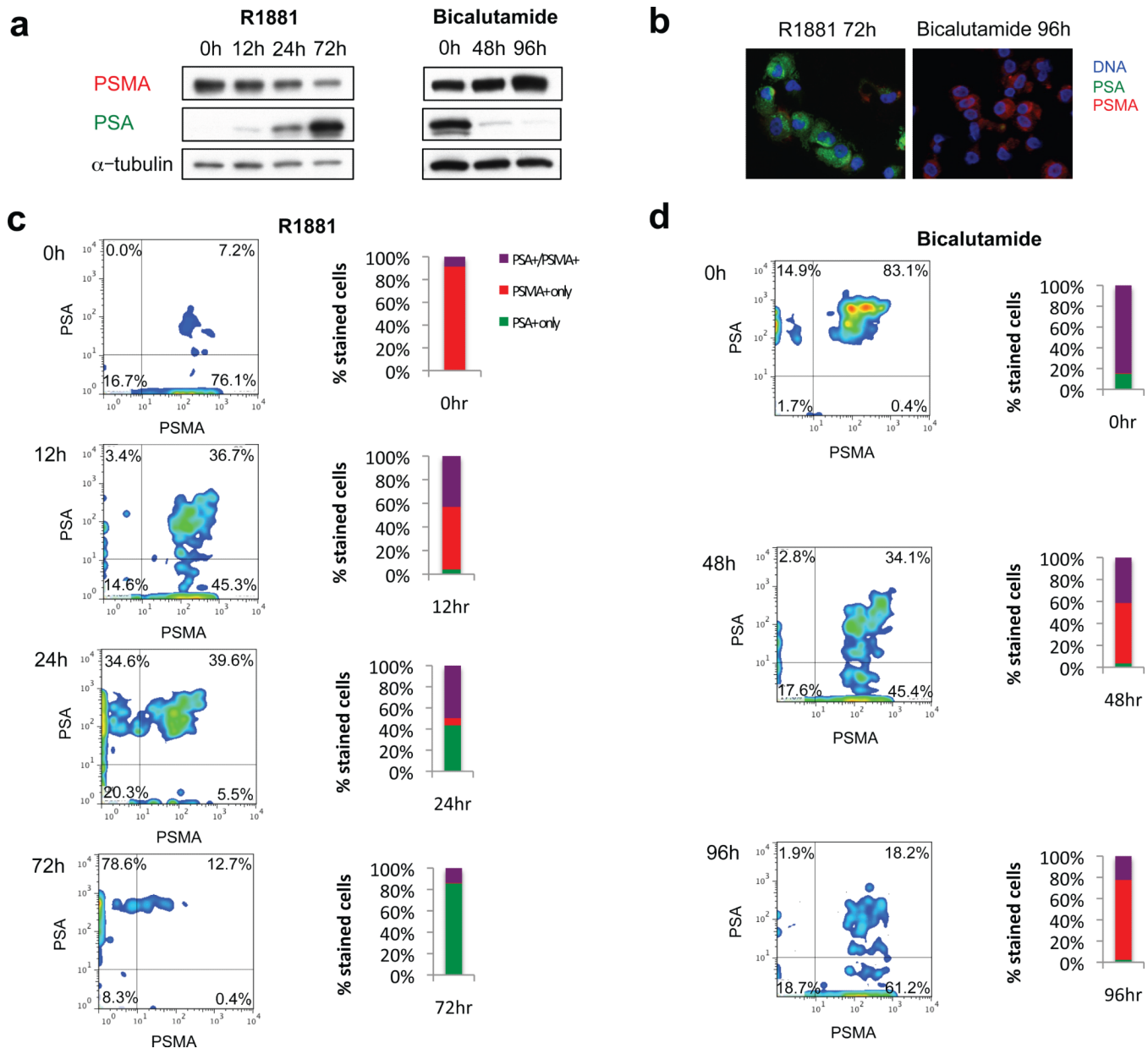

Figure 1.

Multiparameter single cell immunofluorescence assay to measure changes in AR activity in cultured prostate cancer cells. (**a**) Western blot for PSA, PSMA, and alpha-tubulin in LNCaP cells treated with 1 nM R1881 after being cultured under androgen-deprived conditions (left panel), or treated with 10μM bicalutamide after being cultured under standard conditions (right panel). (**b**) Merged immunofluorescence images of LNCaP cells dual stained with antibodies against PSA (green) and PSMA (red) after treatment with 1 nM R1881 or 10 μM bicalutamide. (**c**) Pseudocolor density plots of multiparameter immunofluorescence profiles of LNCaP cells treated with 1 nM R1881, imaged using an automated fluorescence microscopy scanning system. *X*- and *y*- axes represent “area-pixel” single cell signal intensity measurements for PSMA and PSA, respectively. The total fraction of PSA+/PSMA- (AR-on), PSA-/PSMA+ (AR-off), and PSA+/PSMA+ (AR-mixed)

cells is shown in the bar graph. (**d**) Comparable analysis for LNCaP cells treated with 10 μM bicalutamide after being cultured under standard conditions.

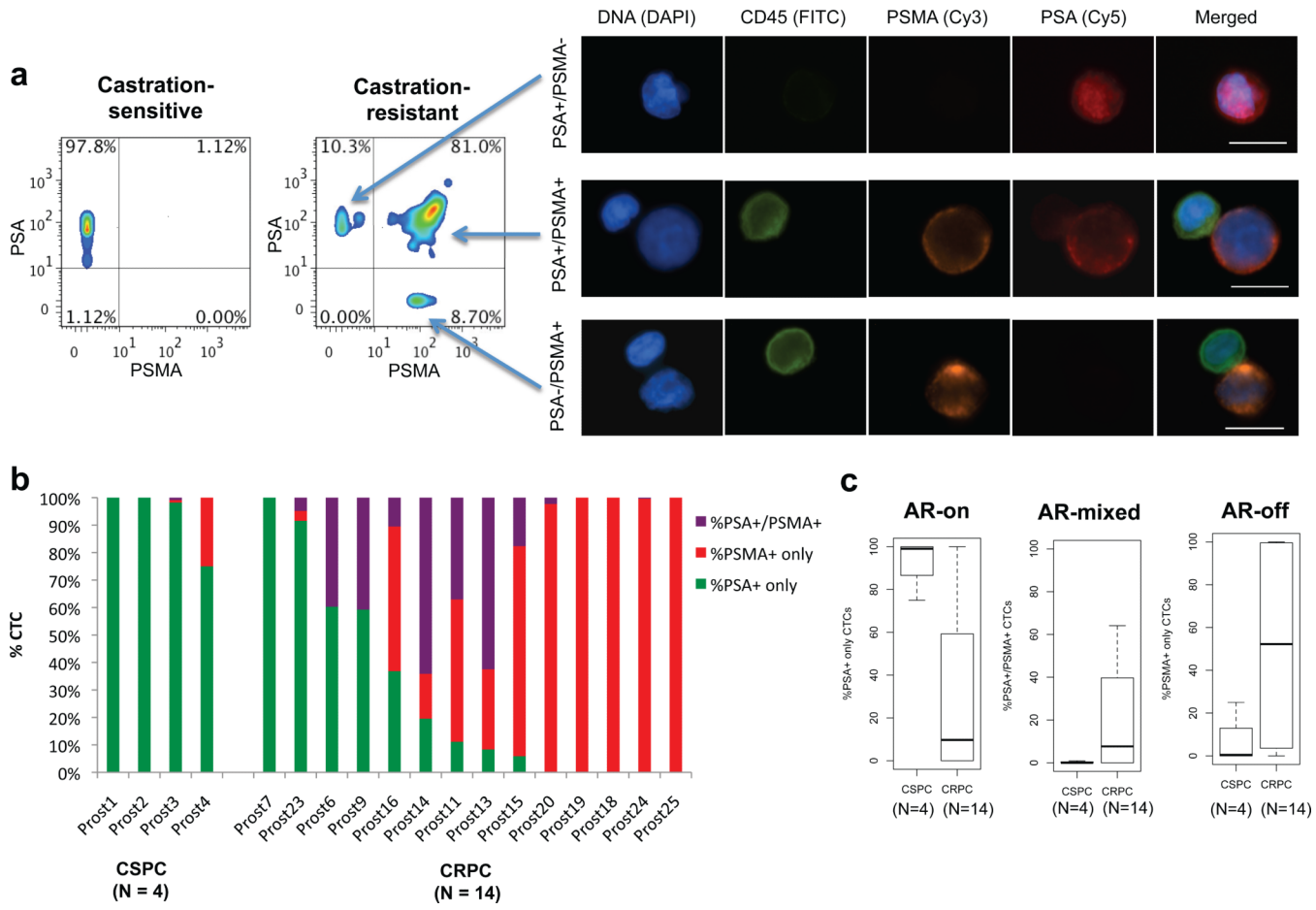

Figure 2.

Single cell measurements of AR signaling identify predominantly AR-on CTCs in castration-sensitive prostate cancer versus heterogeneous signatures in castration-resistant prostate cancer. (**a**) Pseudocolor density plots of multiparameter immunofluorescence profiles of CTCs from patient with castration-sensitive prostate cancer (left panel) and castration-resistant prostate cancer (right panel). *X*- and *y*- axes represent “area-pixel” single cell signal intensity measurements for PSMA and PSA, respectively. Representative images are depicted of an “AR-on” (PSA+/PSMA-) CTC (top row on right), an “AR-mixed” (PSA +/PSMA+) CTC (middle row), and an “AR-off” (PSA-/PSMA+) CTC (bottom row), with CD45 (FITC), PSMA (Cy3), and PSA (Cy5). Contaminating CD45+ leukocytes are depicted for comparison in the middle and bottom rows. Scale bars, 10 μm. (**b**) Bar graphs showing proportional distribution of AR signaling phenotypes in CTCs from patients with CSPC or CRPC prior to initiation of therapy. Patient samples are ordered according to relative percentage of “AR-on” %PSA+ only CTCs. (**c**) Box plots demonstrating the relative proportions of AR signaling phenotypes in CTCs from patients with CSPC compared to CRPC prior to initiation of therapy ($P = 0.012$ for %PSA+/PSMA-; $P = 0.071$ for %PSA+/PSMA+; $P = 0.076$ for %PSA-/PSMA+).

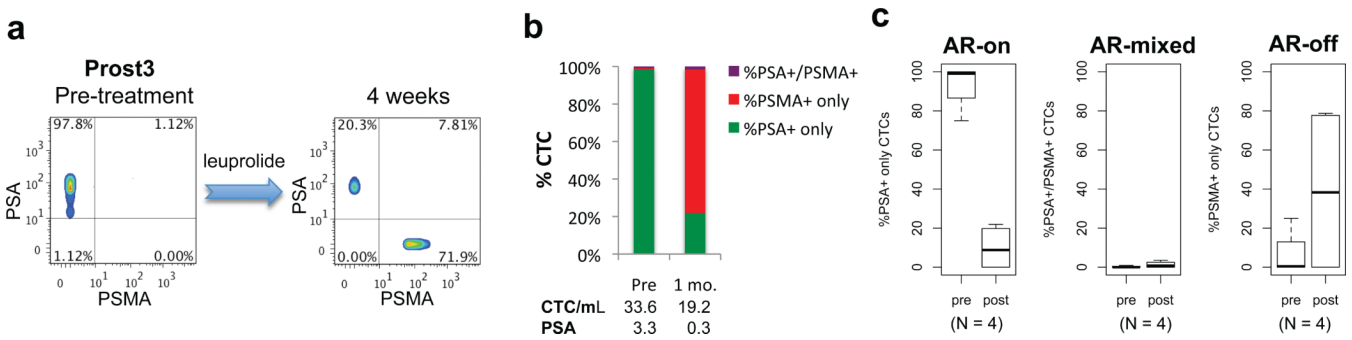

Figure 3.

ADT-induced AR signaling changes in CTCs from patients with castration-sensitive metastatic prostate cancer. (**a**) Pseudocolor density plots of multiparameter immunofluorescence AR signaling profiles of CTCs in a patient with castration-sensitive prostate cancer before and after ADT with leuprolide showing transformation of CTCs from the “AR-on” (PSA+/PSMA-) phenotype to the “AR-off” (PSA-/PSMA+) phenotype. (**b**) Bar graphs showing proportional distribution of AR signaling phenotypes in CTCs from this patient before and after ADT. Corresponding CTC numbers and serum PSA levels are shown for pretreatment (pre) and after therapy. (**c**) Box plots showing composite data for relative proportions of AR signaling phenotypes in CTCs from patients with castration-sensitive prostate cancer ($n = 4$) pretreatment and after 4 weeks of ADT ($P = 0.028$ for %PSA+/PSMA-; $P = 0.41$ for %PSA+/PSMA+; $P = 0.64$ for %PSA-/PSMA+).

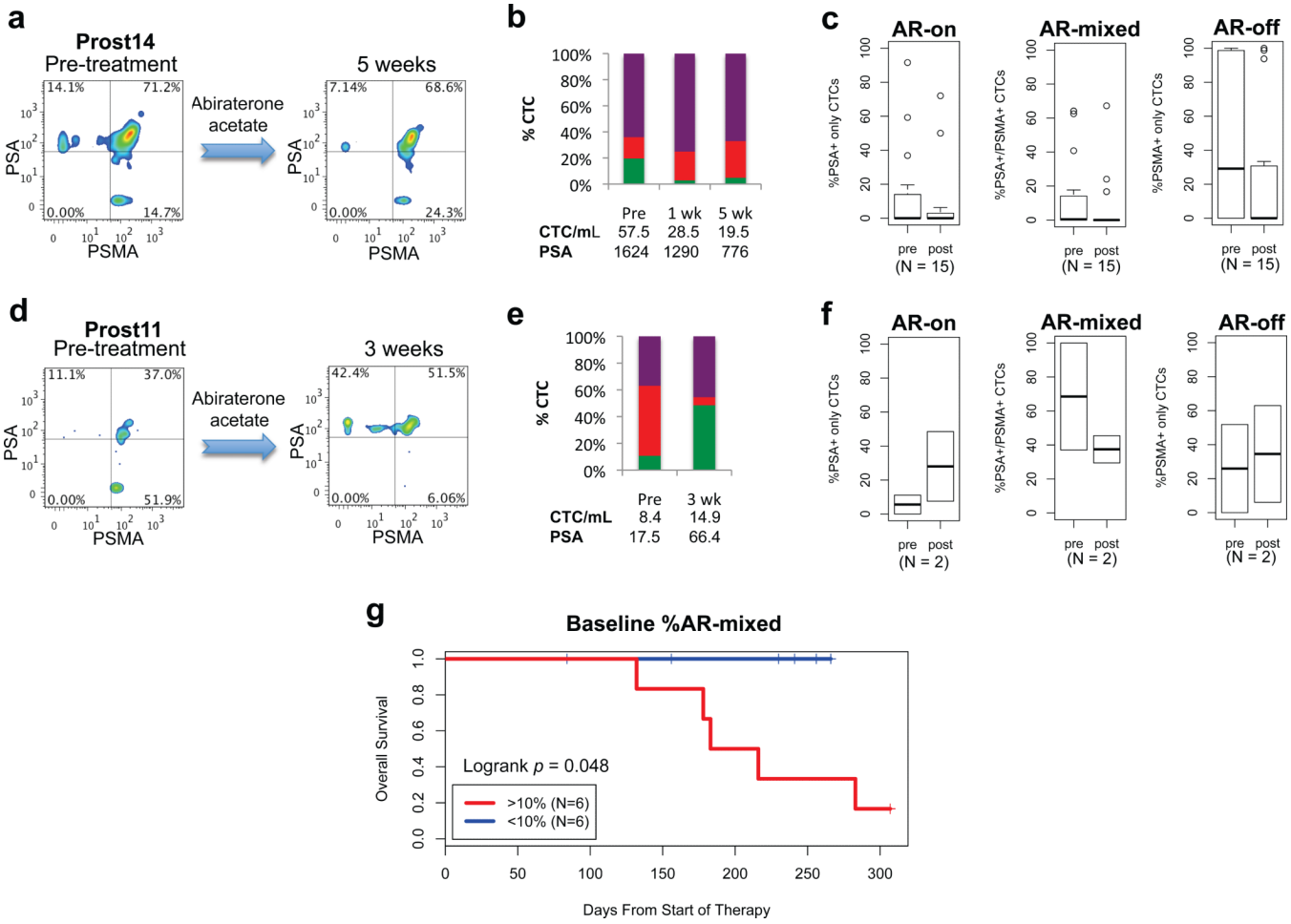

Figure 4.

AR signaling in CTCs from CRPC patients treated with abiraterone acetate. (**a**) Pseudocolor density plots of multiparameter immunofluorescence AR signaling profiles of CTCs in a patient with CRPC, showing a decrease in the proportion of PSA+/PSMA- "AR-on" CTCs after initiation of abiraterone acetate. (**b**) Bar graphs depicting the results for this patient at serial time points following treatment. Corresponding CTC numbers and serum PSA levels are shown for pretreatment (pre) and at weeks following therapy. (**c**) Box plots showing composite data for relative proportions of AR signaling phenotypes in CTCs from patients that exhibit stable or declining proportion of "AR-on" CTCs after initiation of therapy (P = 0.56 for %PSA+ only; P = 0.12 for %PSA+/PSMA+; P = 0.14 for %PSMA+ only). (**d**) Increase in the proportion of PSA+/PSMA- "AR-on" CTCs observed in a patient with CRPC after treatment with abiraterone acetate. (**e**) Bar graphs depicting the results for this patient. (**f**) Box plots showing composite data for relative proportions of AR signaling phenotypes in CTCs from patients that exhibit an increasing proportion of "AR-on" CTCs after initiation of therapy (P = 0.67 for %PSA+ only; P = 0.67 for %PSA+/PSMA+; P = 0.67 for %PSMA+ only). (**g**) Kaplan-Meier curves for overall survival in patients with CRPC treated with abiraterone acetate, according to baseline percentage of >10% "AR-mixed" CTCs (red) versus <10% "AR-mixed" CTCs (blue) (logrank P = 0.048).